

A Network Slicing Algorithm for 5G Vehicular Networks

Emmanouil Skondras¹, Angelos Michalas², Dimitrios J. Vergados³, Emmanouel T. Michailidis⁴, Nikolaos I. Miridakis⁵

¹Department of Informatics, University of Piraeus, Piraeus, Greece, Email: skondras@unipi.gr

²Department of Electrical and Computer Engineering, University of Western Macedonia, Kozani, Greece, Email: amichalas@uowm.gr

³Department of Informatics, University of Western Macedonia, Kastoria, Greece, Email: dvergados@uowm.gr

⁴Department of Electrical and Electronics Engineering, University of West Attica, Egaleo, Athens, Greece, Email: emichail@uniwa.gr

⁵Department of Informatics and Computer Engineering, University of West Attica, Egaleo, Athens, Greece, Email: nikozm@uniwa.gr

Abstract—Fifth generation (5G) vehicular networks support various services with strict Quality of Service (QoS) constraints. Network access technologies such as the LTE Vehicle to Everything (LTE-V2X) and the IEEE 802.11ac/ax provide network access to users, while Software Defined Networking (SDN) provides centralized control of the heterogeneous network environment. In this environment, each vehicle could serve multiple passengers with multiple services. Therefore, the design of efficient resource allocation schemes for 5G vehicular infrastructures is needed. This paper describes a network slicing scheme for 5G systems that aims to optimize the performance of modern vehicular services. In particular, the throughput that each user obtains for his services is considered. If the available connection throughput is above a predefined service threshold, then the necessary telecommunication resources from the current Point of Access (PoA) are allocated to support the user's services. On the contrary, if the available connection throughput is lower than the aforementioned threshold, additional resources from a Virtual Resource Pool (VRP) located at the SDN controller are committed by the PoA in order to satisfy the required services. Performance evaluation shows that the suggested method outperforms existing algorithms in terms of throughput, end to end delay, jitter and packet loss ratio.

Index Terms—5G Vehicular Networks, LTE Vehicle to Everything (LTE-V2X), IEEE 802.11ac/ax, Network Slicing, Resource Virtualization

I. INTRODUCTION

Nowadays, 5G Network Slicing is receiving increased attention from both the research and the industrial communities. Radio Access Network (RAN) virtualization [1] is one of the most important challenges that have appeared. Many solutions allow spectrum division while providing isolation of radio resources. However, the usage of the available resources is not always efficient and reliable. Another challenge for RAN virtualization is the ability to have multiple Radio Access Technologies (RATs), namely a heterogeneous RAN, as they are essential for 5G networks.

Regarding the network access technologies that can be used for implementing network slicing, the Long Term Evolution (LTE), the IEEE 802.11ac and the IEEE 802.11ax have obtained increased research interest.

Specifically, the LTE-A Pro FD-MIMO (rel. 15) [2], [3] allows the existence of up to 64-element antennas in each evolved NodeB (eNB) enhancing the capacity of the access network. In such an architecture, information is transmitted in frames of 10ms of length and every frame is split into 10 sub-frames of 1 Time Transmission Interval (TTI) of length. The minimum resource which can be allocated for transmission is called Resource Block (RB). RBs are allocated to users in each TTI and the number of available RBs per TTI depends on the system bandwidth. In particular, flexible component carrier bandwidths from 1.4 up to 20MHz are allowed, while 100 RBs are available for allocation per component carrier in the case of 20MHz bandwidth. Furthermore, multiple antennas per eNB can further increase the available bandwidth, allowing the implementation of Ultra Dense Networking (UDN) [4] architectures. Also, the LTE Vehicle to Everything or LTE-V2X [2] technology allows the implementation of the aforementioned characteristics in Road Side Units (RSU) to support vehicular infrastructures.

In addition, the IEEE 802.11ac Very High Throughput (VHT) technology, which is also called the fifth generation of WiFi networks (WiFi 5), is based upon the Orthogonal Frequency Division Multiplexing (OFDM) [5] technique. Regarding the specifications of the 802.11ac, up to 80 MHz channel bandwidth and Multi User-Multiple Input Multiple Output (MU-MIMO) [6] with up to 8 spatial streams are supported. Furthermore, the IEEE 802.11ax technology, which is also called as the sixth generation of WiFi networks (WiFi 6), applies Orthogonal Frequency Division Multiple Access

978-1-6654-0032-9/21/\$31.00 ©2021 IEEE

(OFDMA) [7] which allows each subcarrier to be further divided into individual portions called Resource Units (RUs) and can be assigned to users.

In 5G vehicular networks, vehicular users use On-Board Units (OBUs) or smart mobile devices with computational, storage and communication resources. This equipment communicates with each other as well as with access network infrastructures consisting of LTE-A Pro FD-MIMO macrocells, LTE V2X RSUs as well as other network access technologies. In a such architecture, each Point of Access (PoA) can interact with a Cloud infrastructure which offers a variety of vehicular services with strict Quality of Service (QoS) constraints. Thus, vehicles can provide various cloud services to their passengers, while at the same time each vehicle could serve many passengers with different services and various requirements. To address this situation, efficient resource allocation mechanisms should be implemented. This paper describes a novel network slicing scheme for 5G vehicular networks. The proposed scheme aims to optimize the performance of modern vehicular services such as Voice over IP (VoIP), Autonomous Navigation (ANav), Conversational Video (CV) and Web Browsing (WB). The throughput that each user receives for his services is considered. If the throughput obtained from the PoA attains a predefined service threshold, then only resources from the current PoA are allocated. On the contrary, if the available connection throughput is lower than the aforementioned threshold, then additional communication resources from a Virtual Resource Pool (VRP) are committed by the PoA so as to achieve the required throughput. The VRP entity is maintained by a Software Defined Network (SDN) controller and includes RBs that can be shared between the available PoAs.

The remainder of the paper is as follows: In section II the related research literature is revised, while section III presents the proposed algorithm for performing network slicing on 5G vehicular networks. Section IV presents the simulation setup and results, while section V presents the evaluation of the scheme in real world test cases using a testbed implemented in controlled laboratory environment. Finally, section VI concludes the discussed work.

II. STATE OF THE ART

As the International Telecommunication Union (ITU) and the Fifth Generation Public Private Partnership (5G-PPP) have specified, 5G vehicular networks support three main categories of modern communications, namely the Enhanced Mobile Broadband, the Massive Machine-type Communications and the Critical Communications (or Low Latency Communications) [8]. In order to meet the new standards and requirements, many 5G architectures have been proposed, each serving a different use case. In addition, according to the Next Generation Mobile Network Alliance (NGMN), network architecture should be approached with more flexible and efficient techniques such as Network Slicing

Initially, only Core Network (CN) slicing [9] was proposed in the academic and industrial domain. Thereafter, the NGMN

also supported End-to-End (E2E) slicing [10] in order to enhance both the performance of the Radio Access Network (RAN) and the Core Network (CN). Specifically, the NGMN proposes a three-layer network management architecture, which consists of the Infrastructure Resource layer, the Business Enablement layer and the Business Application layer. According to the NGMN, a Network Slice represents an instance of a service consisting of a specific structure, configuration and workflow. Each Slice employs multiple instances of logical subnetworks. Each subnetwork fulfils the diverse functions and requirements requested by the particular service. The whole process is organized by an End-to-End (E2E) MANO entity [11].

Additionally, the architecture proposal of the 5G Infrastructure Public Private Partnership (5G-PPP) describes in detail the relations among the components of the 5G network. Specifically, the proposed architecture consists of five different layers namely the Infrastructure, the Network Function, the Orchestration, Business Function and the Service Layer. In 5G-PPP the MANO entity consists a separate layer. Furthermore, the Business Application layer of the NGMN architecture has been replaced in the 5G-PPP by two separate layers, namely the Business Function layer and the Service layer.

In [12] the guidelines of the ITU, the NGMN and the 5G-PPP are considered and a three-layer framework for Network Slicing implementation is proposed. Specifically, the framework consists of the Service, the Network Function and the Infrastructure layers. The service layer can be approached in two ways: Either it defines the service level description by a set of SLA requirements and services, or it defines a composite structure identifying the functions and RATs that should be used by the slice. The difference between the two lies in the process of the slice generation. In the first scenario, implementation necessitates the application of efficient operations to meet the requirements described. In the second scenario the slice will be implemented in a simpler way however it might be less effective.

Subsequently, the Network Function layer includes both the control and the user planes of the network architecture. Specifically, it includes every operation that has to do with the configuration of the network functions and data forwarding.

The Infrastructure layer refers to the physical resources of both the Radio Access Network (RAN) and the Core Network (CN). Also, it implements functionalities for the management and the allocation of the network resources.

Furthermore, in this framework a MANO entity coexists that converts use cases and service models into network slices using the network functions. The MANO entity links the use cases and service models to infrastructure resources, while at the same time it keeps configuring and monitoring each slice during its life cycle.

Additionally to the aforementioned works, several network slicing schemes have been proposed from the research literature.

In [13] the Reliable Software-Defined RAN (RSDR) scheme for network slicing is proposed. In this scheme, for the allo-

cation of RBs to the available slices, an improved version of the Round Robin (RR) algorithm [14] is applied. Specifically, a weighting value is calculated for each slice in each TTI and slices with higher weight have priority against others to the allocation.

In [15] three network slicing methods are studied. In the first one, which is called the Static Allocation (SA) method, the required number of RBs is estimated for each slice considering its service constraints. Subsequently, each slice allocates its RBs to vehicular users, by applying the Proportional Fairness (PF) [16] resource allocation algorithm. In the second method called Allocation of Ordered Slices (AOS), slices are prioritized. The requirements of slices with higher priority are processed first while the PF algorithm is applied to allocate RBs to the users of each slice. Finally, the third method called Impartial Allocation (IA) is an extension of the AOS method. In this approach, each slice selects which RBs will be allocated to its users, considering the channel quality of each RB. Thus, slices with higher priority allocate RBs with higher channel quality, thus increasing the quality of their services.

In [17] a network slicing scheme for 5G-V2X systems is proposed. In particular, two slices are created, namely the autonomous driving slice and the infotainment slice. The autonomous driving slice is responsible for allocating communication resources for the transmission of road safety information, while the infotainment slice supports video streaming services. Both slices use the PF algorithm for the allocation of their communication resources to each user service.

III. THE PROPOSED NETWORK SLICING SCHEME

The proposed scheme defines the two layer network architecture presented in figure 1. The architecture consists of the Local Resource Allocation (LRA) layer and the Shared Resource Allocation (SRA) layer.

The LRA layer includes a set of Points of Access (PoAs) that provide network access to vehicular users, while each PoA has a set of communication resources (CRs). A variable $CR_k^{rem}(t)$ indicates the remaining resources of the k^{th} PoA during the t^{th} Transmission Time Interval (TTI). Also, the resources of the PoAs are organized into two subsets, which are called Local CRs (LCRs) and Shared CRs (SCRs).

The SRA layer includes an SDN controller which maintains a Virtual Resource Pool (VRP). Specifically, the VRP includes all the SCRs that are available on the PoAs.

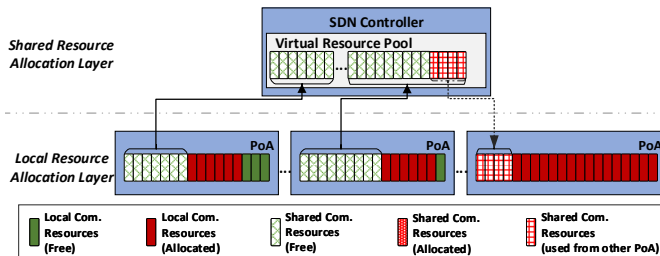


Fig. 1: The design of the proposed Network Slicing architecture.

A set of services per vehicle, require resources to satisfy their constraints. For each service, a variable $th^{threshold}$ indicates the minimum acceptable throughput for the service. Also, the $th_u^{estimated}(t^n)$ indicator is defined, determining the available throughput for user u during the upcoming t^n TTI that is the next TTI for which RBs will be allocated.

The $th_u^{estimated}(t^n)$ parameter is estimated using formula 1, where $\mu(t^t)$ represents the estimated throughput per RB and $r_{available}^n$ is the number of the RBs that are available for allocation.

$$th_{m,u}^{estimated}(t^n) = \mu(t^n) \cdot r_{available}^n \quad (1)$$

If the estimated $th_u^{estimated}(t^n)$ is less than the $th^{threshold}$ threshold value, the service requirements can be satisfied from the remaining LCRs that exist in the current RSU. However, if the estimated $th_u^{estimated}(t^n)$ is higher than the $th^{threshold}$ value, the service requirements cannot be satisfied from the remaining LCRs and, thus, SCRs are also committed for the user.

For the allocation of the committed number of resources to the services of each user an improved version of the Modified Largest Weighted Delay First (MLWDF) [18] algorithm, which is called MLWDF-Advanced (MLWDF-A) is proposed. Specifically, the MLWDF metric is improved by taking into consideration the past average values concerning the throughput, the packet transfer delay, the jitter and the packet loss ratio, as presented in formula 2, where the $D_{HOL,i}$ represents the head of line delay, $d(t-1)$ is the normalized past average packet transfer delay, $j(t-1)$ is the normalized past average jitter and $pl(t-1)$ is the normalized past average packet loss ratio. Also, the α_i value is determined by formula 3, where δ_i is the target packet loss ratio and τ_i is the constraint of the packet transfer delay. The use of the QoS aware scheduling metric of the MLWDF-A, allows the optimal allocation of the committed RBs to user services and improves the QoS that each service perceives.

$$m_{i,k}^{MLWDF-A} = a_i \cdot D_{HOL,i} \cdot \frac{\mu_k^i(t)}{th^i(t-1)} \cdot d(t-1) \cdot j(t-1) \cdot pl(t-1) \quad (2)$$

$$\alpha_i = -\frac{\log \delta_i}{\tau_i} \quad (3)$$

IV. SIMULATION SETUP AND RESULTS

The design of the proposed scheme is evaluated using simulations. Specifically, the 5G network topology presented in figure 2 is implemented using the Network Simulator 3 (NS3) [19]. It includes a Fog infrastructure, as well as a Cloud infrastructure.

The Fog infrastructure consists of 7 LTE-V2X RSUs with 4 antennas each. The spectrum of each RSU is presented in table I. On the other hand, the Cloud infrastructure includes a set of Virtual Machines (VMs) providing services such as Voice over IP (VoIP), Autonomous Navigation (ANav), Conversational Video (CV) and Web Browsing (WB). Table

TABLE I: The spectrum each LTE V2X RSU downlink.

| Network | Downlink Spectrum in MHz (LTE Band) | | | |
|---------------|-------------------------------------|----------------|----------------|----------------|
| | Antenna 1 | Antenna 2 | Antenna 3 | Antenna 4 |
| LTE-V2X RSU 1 | 3510-3515 (22) | 3515-3520 (22) | 3520-3525 (22) | 3525-3530 (22) |
| LTE-V2X RSU 2 | 3530-3535 (22) | 3535-3540 (22) | 3540-3545 (22) | 3545-3550 (22) |
| LTE-V2X RSU 3 | 3550-3555 (22) | 3555-3560 (22) | 3560-3565 (22) | 3565-3570 (22) |
| LTE-V2X RSU 4 | 3570-3575 (22) | 3575-3580 (22) | 3580-3585 (22) | 3585-3590 (22) |
| LTE-V2X RSU 5 | 2110-2115 (1) | 2115-2120 (1) | 2120-2125 (1) | 2125-2130 (1) |
| LTE-V2X RSU 6 | 2130-2135 (1) | 2135-2140 (1) | 2140-2145 (1) | 2145-2150 (1) |
| LTE-V2X RSU 7 | 2150-2155 (1) | 2155-2160 (1) | 2160-2165 (1) | 2165-2170 (1) |

TABLE II: The 5QI value and the corresponding constraints for each service

| Service | 5QI Value | Resource Type | Priority Level | Packet Delay Budget | Packet Error Rate |
|------------------------------|-----------|--------------------|----------------|---------------------|-------------------|
| Voice over IP (VoIP) | 1 | GBR | 20 | 100 ms | 10^{-2} |
| Autonomous Navigation (ANav) | 81 | Delay Critical GBR | 11 | 5 ms | 10^{-5} |
| Conversational Video (CV) | 2 | GBR | 40 | 150 ms | 10^{-3} |
| Web Browsing (WB) | 6 | Non-GBR | 60 | 300 ms | 10^{-6} |

It presents the 5QI value assigned to each service, along with the corresponding constraints as they are defined in the 5GPP specifications for 5G communications [20].

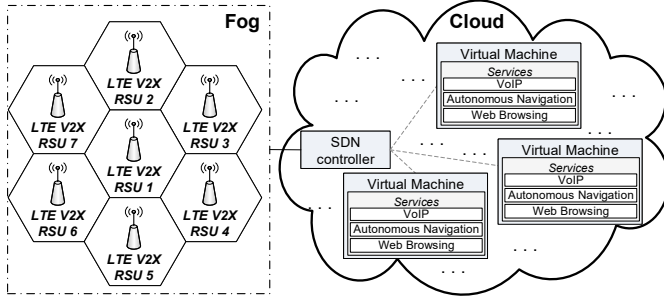


Fig. 2: The simulated topology.

A set of up to 50 vehicles move inside the network access environment of the LTE-V2X RSU 1. Each vehicle receives 1 flow for each of the services of table II. Furthermore, an OpenFlow SDN controller [21] provides centralized control of the entire system, maintaining the Virtual Resource Pool (VRP) with the Shared CRs (SCRs). Table III presents the simulation parameters.

The proposed scheme is compared with the RR and RSDR algorithms described in [13]. The parameters considered for the performance evaluation include the throughput, the end to end delay, the jitter and the packet loss ratio. As observed from the simulation results, the proposed scheme outperforms both the RR and the RSDR algorithms since each RSU that requires increased number of communication resources to satisfy the constraints of user services, can commit additional RBs from the Virtual Resource Pool. In particular, as presented in figure 3 the proposed scheme succeeds up to $1.5Mbps$ higher throughput than those succeeded from the other two schemes for the VoIP service slice, while at the same time

TABLE III: The simulation parameters.

| Parameter | Value |
|----------------------------------|---|
| Simulation duration | 18000 seconds (5 hours) |
| Networks count | LTE-V2X RSUs: 7 |
| Cells radius | LTE-V2X cell: 100 meters |
| Networks positions & frequencies | See Appendix B |
| Vehicles count | Up to 50 on LTE-V2X RSU 1 |
| Services | Voice over IP (VoIP) using G.729 codec [22] Autonomous Navigation (ANav) Conversational Video (CV) Web Browsing (WB) |

up to $6.6ms$, $0.8ms$ and 14% lower values are observed for both the packet transfer delay, the jitter and the packet loss ratio factors, respectively. In similar, figures 4, 5 and 6 present the corresponding results for the ANav, the CV and the WB services, respectively. As it can be observed, in the case of the ANav service slice the proposed scheme succeeds up to $20Mbps$ higher throughput, while at the same time it succeeds up to $2.5ms$, $0.3ms$ and 69% lower values for the delay, the jitter and the packet loss ratio factors, respectively. Also, similar results are observed in the case of the CV service slice, which requires the highest throughput from the rest of the considered services. In this case, up to $63Mbps$ higher throughput is observed in the proposed methodology at the same time the values for the delay, the jitter and the packet loss ratio are up to $73ms$, $23ms$ and 84% lower than those of the other schemes, respectively. Also, for the WB service slice, the proposed scheme succeeds up to $47.7Mbps$ higher throughput and up to $222ms$, $27.7ms$ and 99.3% lower values for the delay, the jitter and the packet loss ratio, respectively. Finally, it has to be noted that the proposed scheme satisfies the packet transfer delay and the packet loss ratio constraints for the entire services, while at the same time the other schemes does not satisfy them in cases where an increased number of vehicles require resources from the RSU. Thus, in cases where either the RR or the RSDR scheme is used, critical information may be lost leading to undesirable situations (e.g. road accident in case of ANav services).

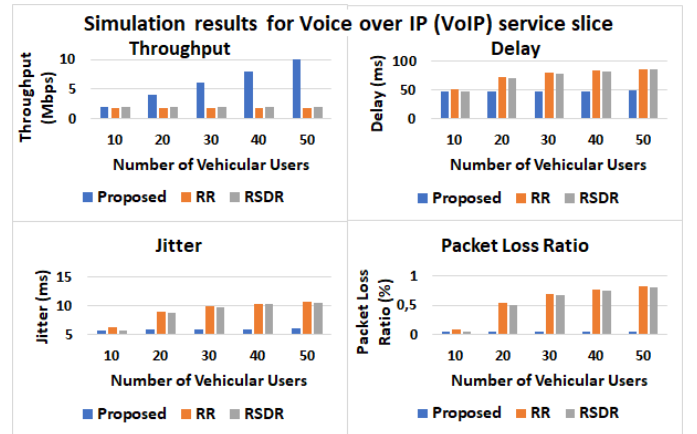


Fig. 3: The performance evaluation results of VoIP services.

V. TESTBED DEPLOYMENT AND RESULTS

For the evaluation of the proposed scheme in real world scenarios, a testbed is implemented in a controlled laboratory environment. Figure 7 presents the design of the implemented network architecture which is built using equipment from the TP-Link Omada Cloud SDN platform [23]. Specifically, the network access environment consists of a TP-LINK EAP245 indoor MU-MIMO Access Point (AP) [24], 3 TP-LINK EAP225 indoor MU-MIMO APs [25] and 3 TP-LINK EAP225 MU-MIMO outdoor APs [26]. Also, a Huawei RH2288H V3 rack server [27] implements a Cloud infrastructure with a set of Virtual Machines (VMs) providing VoIP, ANav, CV and

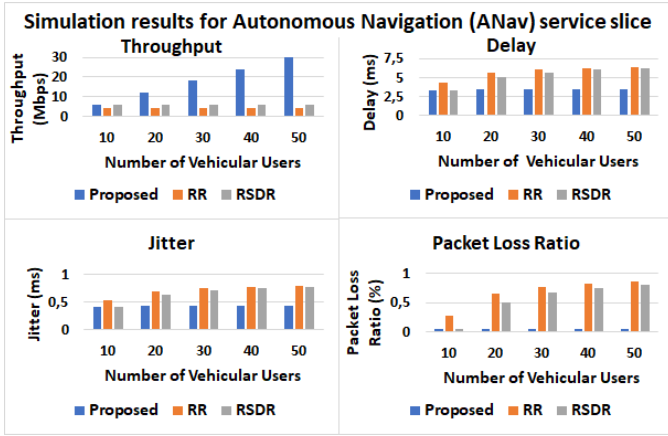


Fig. 4: The performance evaluation results of Autonomous Navigation services.

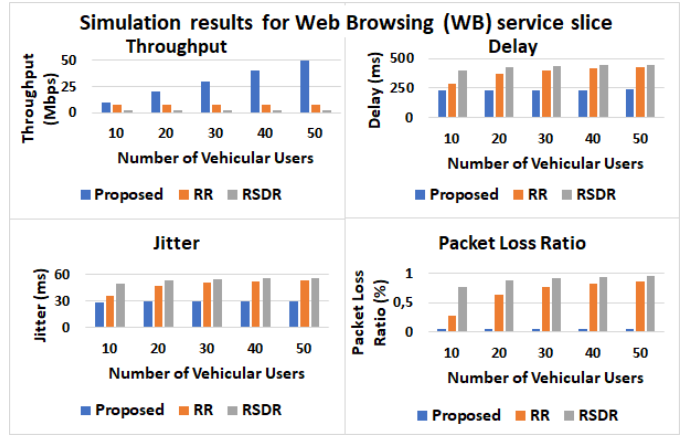


Fig. 6: The performance evaluation results of Web Browsing services.

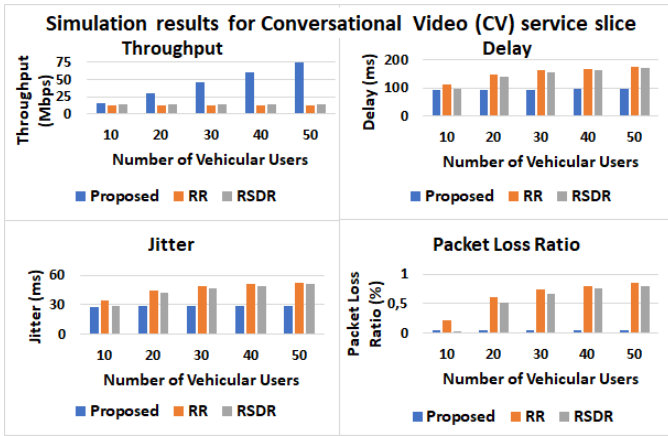


Fig. 5: The performance evaluation results of Conversational Video services.

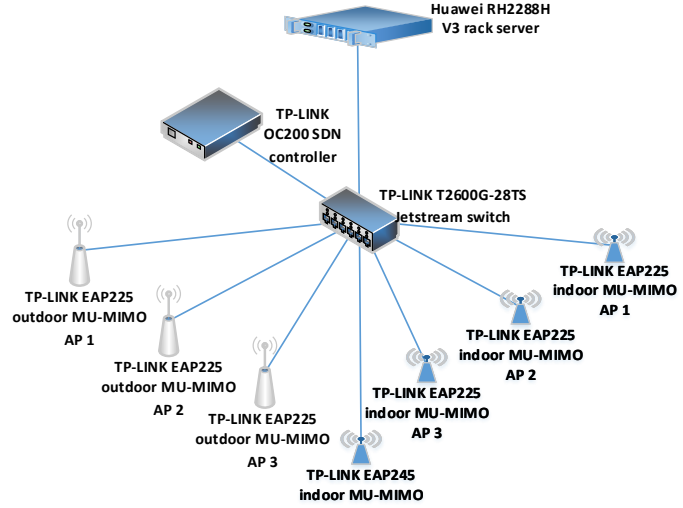


Fig. 7: The architecture of the implemented testbed.

WB services. The APs and VMs are connected to a TP-LINK T2600G-28TS Jetstream switch [28], while a TP-LINK OC200 cloud controller [29] along with the TP-Link Omada controller software [30] provide centralized control to the entire testbed architecture. Additionally, up to 20 Android Virtual Devices (AVDs) [31] are connected to the TP-LINK EAP245 indoor MU-MIMO AP, while each AVD receives one flow from each service. Table IV presents the technical parameters of the implemented testbed.

As it is presented in figure 8 the proposed scheme succeeds up to $180kbps$ higher throughput than the one succeeded from the other two schemes for the VoIP service slice, while at the same time up to $6.7ms$, $0.84ms$ and 14% lower values are observed for both the end to end delay, the jitter and the packet loss ratio factors, respectively. In similar, figures 9, 10 and 11 present the corresponding results for the ANav, the CV and the WB services, respectively. Specifically, in the case of the ANav service slice the proposed scheme succeeds up to $7.2Mbps$ higher throughput, while at the same time up to $2ms$, $0.25ms$ and 60% lower values in respect to the delay, the jitter and the packet loss ratio factors. Also, similar results are observed in the cases of the CV and the WB service slices, where the proposed scheme succeeds up to $682Mbps$ and $96Mbps$

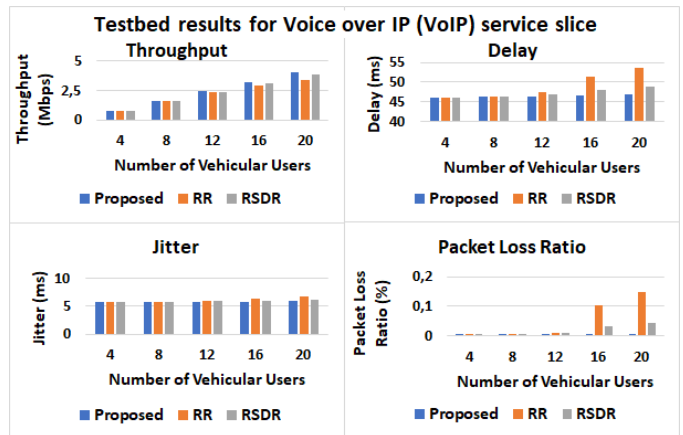


Fig. 8: The testbed results of VoIP services.

higher throughput, respectively, as well as lower values for the delay, the jitter and the packet loss ratio parameters.

TABLE IV: The testbed parameters.

| Access Points (APs) | | | | | | | | | | | | | |
|---------------------|---------|---------------|---------|-----------|-------------------|--------------|----------|---------------|---------|-----------|-------------------|--------------|----------|
| Model | Type | Used standard | Channel | Frequency | Default Bandwidth | Max TX rate* | TX power | Used Standard | Channel | Frequency | Default Bandwidth | Max TX rate* | TX power |
| TP-LINK EAP245 AP | Indoor | IEEE 802.11n | 1 | 2412 MHz | 40 MHz | 300 Mbps | 15 dBm | IEEE 802.11ac | 36 | 5180 MHz | 80 MHz | 1300 Mbps | 23 dBm |
| TP-LINK EAP225 AP1 | Indoor | IEEE 802.11n | 7 | 2442 MHz | 40 MHz | 300 Mbps | 15 dBm | IEEE 802.11ac | 100 | 5500 MHz | 80 MHz | 866.7 Mbps | 23 dBm |
| TP-LINK EAP225 AP2 | Indoor | IEEE 802.11n | 1 | 2412 MHz | 40 MHz | 300 Mbps | 15 dBm | IEEE 802.11ac | 64 | 5320 MHz | 80 MHz | 866.7 Mbps | 23 dBm |
| TP-LINK EAP225 AP3 | Indoor | IEEE 802.11n | 7 | 2442 MHz | 40 MHz | 300 Mbps | 15 dBm | IEEE 802.11ac | 52 | 5260 MHz | 80 MHz | 866.7 Mbps | 23 dBm |
| TP-LINK EAP245 AP1 | Outdoor | IEEE 802.11n | 7 | 2442 MHz | 40 MHz | 300 Mbps | 20 dBm | IEEE 802.11ac | 52 | 5260 MHz | 80 MHz | 866.7 Mbps | 25 dBm |
| TP-LINK EAP245 AP2 | Outdoor | IEEE 802.11n | 1 | 2412 MHz | 40 MHz | 300 Mbps | 20 dBm | IEEE 802.11ac | 64 | 5320 MHz | 80 MHz | 866.7 Mbps | 25 dBm |
| TP-LINK EAP245 AP3 | Outdoor | IEEE 802.11n | 7 | 2442 MHz | 40 MHz | 300 Mbps | 20 dBm | IEEE 802.11ac | 100 | 5500 MHz | 80 MHz | 866.7 Mbps | 25 dBm |

*Regarding the Default Bandwidth

| Switches | | Ports | | |
|--------------------------------|---|--|------------------------------------|--|
| Model | TP-LINK T2600G-28TS | 24 Gigabit Ethernet ports & 4 Small Form-factor Pluggable (SFP) 4 Gbps ports | | |
| Jetstream | | | | |
| SDN Controllers | | | | |
| Model | Description | | | |
| TP-LINK OC200 | Centralized Management of the Omada Cloud Platform, including the TP-LINK EAP APs | | | |
| Serving Virtual Machines (VMs) | | | | |
| VM count | Operating System | Service Specifications | | |
| | | VoIP data traffic | Autonomous Navigation data traffic | Conversational Video data traffic |
| 10 | Ubuntu 20.04 LTS | 200 kbps (codec: G.729) | 600 kbps | 811 Mbps (8K video with 30 Frames per Second (FPS)) [32] |
| | | Web Browsing data traffic | | |
| | | 8 Mbps | | |

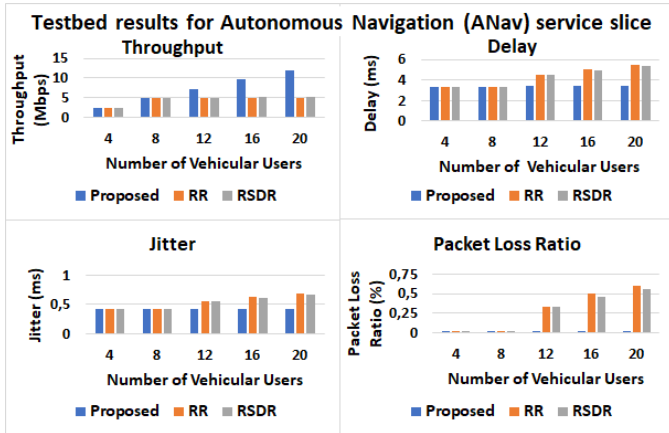


Fig. 9: The testbed results of Autonomous Navigation services.

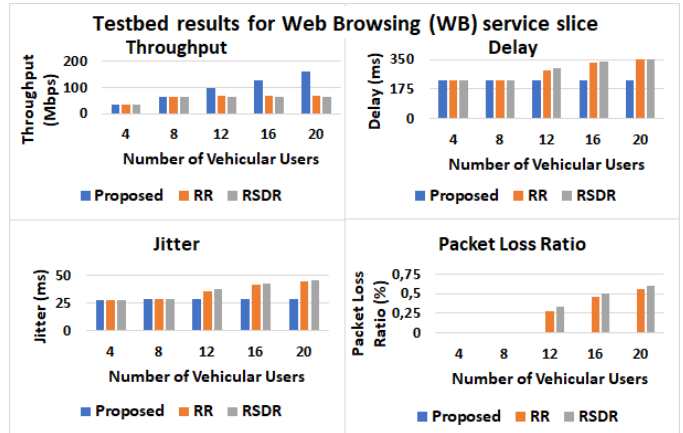


Fig. 11: The testbed results of Web Browsing services.

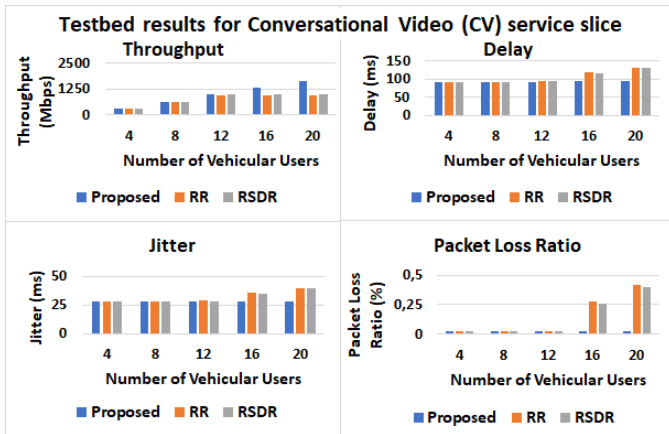


Fig. 10: The testbed results of Conversational Video services.

VI. CONCLUSION

In this paper a network slicing scheme for 5G vehicular networks is described, aiming at the optimization of the performance of vehicular services. Specifically, the throughput that each user obtains for each of his services is considered. If the estimated throughput is lower than a predefined threshold, additional communication resources from a Virtual Resource Pool (VRP) are committed for improving the QoS that the user services receive. The orchestration of the entire proce-

cedure is implemented by a Software Defined Network (SDN) controller. The evaluation of the proposed scheme is performed using simulations, as well as real world test cases in a testbed implemented in a controlled laboratory environment. In both cases, experimental results show that the proposed scheme outperforms existing solutions in terms of end to end delay, jitter, throughput and packet loss ratio.

ACKNOWLEDGEMENTS

This research is funded in the context of the project "A Mobile Edge Computing-Enabled 5G Vehicular Networking Architecture to Support Innovative Services" (MIS 5050174) under the call for proposals "Supporting Researchers with an Emphasis on Young Researchers – Cycle B" (EDULLL 103). The project is co-financed by Greece and the European Union (European Social Fund – ESF) by the Operational Programme Human Resources Development, Education and Lifelong Learning 2014-2020.

REFERENCES

- [1] N. Kazemifard and V. Shah-Mansouri, "Minimum delay function placement and resource allocation for open ran (o-ran) 5g networks," *Computer Networks, Elsevier*, vol. 188, p. 107809, 2021.
- [2] "TR 21.915 (V15.0.0): Digital cellular telecommunications system (Phase 2+) (GSM); Universal Mobile Telecommunications System (UMTS); LTE; 5G; (Rel.15)," *Technical Specification, 3GPP*, 2019.

- [3] R. M. Vaghefi, R. C. Palat, G. Marzin, K. Basavaraju, Y. Feng, and M. Banu, "Achieving phase coherency and gain stability in active antenna arrays for sub-6 ghz fdd and tdd fd-mimo: Challenges and solutions," *IEEE Access*, vol. 8, pp. 152 680–152 696, 2020.
- [4] O. Afolalu and N. Ventura, "Carrier aggregation-enabled non-orthogonal multiple access approach towards enhanced network performance in 5g ultra-dense networks," *International Journal of Communication Systems, Wiley*, vol. 34, no. 4, p. e4701, 2021.
- [5] X. Ma, T. Wang, L. Li, W. Raza, and Z. Wu, "Doppler compensation of orthogonal frequency division multiplexing for ocean intelligent multimodal information technology," *Mobile Networks and Applications*, vol. 25, no. 6, pp. 2351–2358, 2020.
- [6] M. Sakai, K. Kamohara, H. Iura, H. Nishimoto, K. Ishioka, Y. Murata, M. Yamamoto, A. Okazaki, N. Nonaka, S. Suyama *et al.*, "Experimental field trials on mu-mimo transmissions for high shf wide-band massive mimo in 5g," *IEEE Transactions on Wireless Communications*, vol. 19, no. 4, pp. 2196–2207, 2020.
- [7] J. Jiang, Y. Li, L. Chen, J. Du, and C. Li, "Multitask deep learning-based multiuser hybrid beamforming for mm-wave orthogonal frequency division multiple access systems," *Science China Information Sciences*, vol. 63, no. 8, pp. 1–11, 2020.
- [8] J. Navarro-Ortiz, P. Romero-Diaz, S. Sendra, P. Ameigeiras, J. J. Ramos-Munoz, and J. M. Lopez-Soler, "A survey on 5g usage scenarios and traffic models," *IEEE Communications Surveys & Tutorials*, vol. 22, no. 2, pp. 905–929, 2020.
- [9] C. H. T. Arteaga, A. Ordoñez, and O. M. C. Rendon, "Scalability and performance analysis in 5g core network slicing," *IEEE Access*, vol. 8, pp. 142 086–142 100, 2020.
- [10] S. Marinova, T. Lin, H. Bannazadeh, and A. Leon-Garcia, "End-to-end network slicing for future wireless in multi-region cloud platforms," *Computer Networks, Elsevier*, vol. 177, p. 107298, 2020.
- [11] E. P. Neto, F. S. D. Silva, L. M. Schneider, A. V. Neto, and R. Immich, "Seamless mano of multi-vendor sdn controllers across federated multi-domains," *Computer Networks*, vol. 186, p. 107752, 2021.
- [12] X. Foukas, G. Patounas, A. Elmokashfi, and M. K. Marina, "Network slicing in 5g: Survey and challenges," *IEEE Communications Magazine*, vol. 55, no. 5, pp. 94–100, 2017.
- [13] C. Bektas, S. Bocker, F. Kurtz, and C. Wietfeld, "Reliable software-defined ran network slicing for mission-critical 5g communication networks," in *2019 IEEE Globecom Workshops (GC Wkshps)*. IEEE, 2019, pp. 1–6.
- [14] S. Liu, Z. Wang, J. Hu, and G. Wei, "Protocol-based extended kalman filtering with quantization effects: The round-robin case," *International Journal of Robust and Nonlinear Control*, vol. 30, no. 18, pp. 7927–7946, 2020.
- [15] D. Nojima, Y. Katsumata, T. Shimojo, Y. Morihiro, T. Asai, A. Yamada, and S. Iwashina, "Resource isolation in ran part while utilizing ordinary scheduling algorithm for network slicing," in *2018 IEEE 87th Vehicular Technology Conference (VTC Spring)*. IEEE, 2018, pp. 1–5.
- [16] J. Joung, "Random space-time line code with proportional fairness scheduling," *IEEE Access*, vol. 8, pp. 35 253–35 262, 2020.
- [17] H. Khan, P. Luoto, M. Bennis, and M. Latva-aho, "On the application of network slicing for 5g-v2x," in *European Wireless 2018; 24th European Wireless Conference*. VDE, 2018, pp. 1–6.
- [18] L. Priya and K. R. Soundar, "Lte: An enhanced hybrid domain downlink scheduling," *Cognitive Systems Research, Elsevier*, vol. 52, pp. 550–555, 2018.
- [19] "Network simulator 3 (ns3)," <https://www.nsnam.org/>, accessed: 2021.
- [20] "View on 5G Architecture (version 3)," *5G PPP Architecture Working Group*, 2019.
- [21] Y.-h. Kim, J.-M. Gil, and D. Kim, "A location-aware network virtualization and reconfiguration for 5g core network based on sdn and nfV," *International Journal of Communication Systems*, vol. 34, no. 2, p. e4160, 2021.
- [22] R. S. Nur'arifah, D. Perdana *et al.*, "Comparative analysis of codec g. 729 and g. 711 on ieee 802.11 ah with mcs and raw slot change mechanism for voip service," in *2019 4th International Conference on Information Technology, Information Systems and Electrical Engineering (ICITISEE)*. IEEE, 2019, pp. 379–384.
- [23] "Tp-link omada cloud sdn platform," <https://www.tp-link.com/us/omada-sdn/>, accessed: 2021.
- [24] "Tp-link eap245 indoor mu-mimo access point," <https://www.tp-link.com/gr/business-networking/ceiling-mount-ap/eap245/>, accessed: 2021.
- [25] "Tp-link eap225 indoor mu-mimo access point," <https://www.tp-link.com/gr/business-networking/ceiling-mount-ap/eap225/>, accessed: 2021.
- [26] "Tp-link eap225 outdoor mu-mimo access point," <https://www.tp-link.com/gr/business-networking/outdoor-ap/eap225-outdoor/>, accessed: 2021.
- [27] "Huawei rh2288h v3 rack server," <https://support.huawei.com/enterprise/en/intelligent-servers/rh2288h-v3-pid-9901881>, accessed: 2021.
- [28] "Tp-link t2600g-28ts jetstream switch," <https://www.tp-link.com/gr/business-networking/managed-switch/t2600g-28ts/>, accessed: 2021.
- [29] "Tp-link omada oc200 hardware controller," <https://www.tp-link.com/us/business-networking/omada-sdn-controller/oc200/>, accessed: 2021.
- [30] "Tp-link omada software controller," <https://www.tp-link.com/us/support/download/omada-software-controller/>, accessed: 2021.
- [31] "Android virtual devices (avd)," <https://developer.android.com/>, accessed: 2021.
- [32] "Big data video: Top ten most demanding videos," in *White Paper, iLab Video Gen Big Data Team*. Huawei, 2017, pp. 1–25.